Polymerization-Induced Colloidal Assembly and Photonic Crystal Multilayer for Coding and Decoding

*Dongpeng Yang, Yuhang Qin, Siyun Ye, and Jianping Ge**

Photonic crystal (PC) films are prepared by precipitation of colloidal crystal seeds in supersaturated solution of particles, followed by crystal growth and structure fixing with photo-polymerization. As the liquid monomer becomes a solid matrix, the highly concentrated particles are forced to precipitate into colloidal microcrystals in short time, and 'polymerization-induced colloidal assembly' (PICA) is shown to be the major driving force to form colloidal crystals. PICA is intrinsically different from evaporation-induced colloidal assembly, because the seed formation and crystal growth are separated into two independent steps, which makes the synthesis more flexible, controllable, and efficient. The PICA process is capable of quickly producing PC films with an ultra-narrow bandgap, tunable thickness, and large size. Based on these characteristics and the blocking effect of the outer PC layer to the reflection signal of inner layer, a coding–decoding system is developed in which the film's composition and stacking sequence can be identified by its distinctive reflection spectrum.

1. Introduction

Polymeric photonic crystal composites have arouse tremendous enthusiasm because it integrates the fixed stacking of colloidal particles with responsive polymer matrix and then produce many smart materials for sensing, display and printing.[1] The polymer wrapping the photonic crystal (PC) is usually capable of deforming or absorbing chemical substances, which effectively changes its lattice constants, refractive indices and thereby the optical properties, so that the composites can be responsive to many external stimuli such as temperature, light, ions and molecules, mechanic forces and electromagnetic fields. Generally, these PC composites are manufactured in a two-step process including the colloidal assembly and polymerization on preformed template, where the former is often regarded as the bottleneck due to the difficulty in large-scale synthesis.

S. Y. Ye, Prof. J. P. Ge
Department of Chemistry
Shanghai Key Laboratory of Green Chemistry
and Chemical Process
East China Normal University
3663 North Zhongshan Road, Shanghai, 200062, China
E-mail: jpge@chem.ecnu.edu.cn
D. P. Yang, Y. H. Qin
Department of Chemistry
Tongji University
1239 Siping Road, Shanghai, 200092, China

DOI: 10.1002/adfm.201301590

In the past decade, various methods have been investigated for the preparation of high quality colloidal crystals in an efficient and convenient way. In most cases, the assembly is achieved through an external-force driven arrangement of mutually repulsive particles. Sedimentation is the first reported method in which gravity sinks the particles towards the substrate to form colloidal crystals.[2] Another traditional but broadly used technique is dip-coating, which produce PC by pulling out the substrate from colloidal dispersion in a controllable speed, or keeping the substrate untouched and evaporating the solvent.[3] Here, the capillary force makes the particle deposited onto the substrate after a convective assembly. Using highly concentrated colloidal solution as precursor, the colloidal crystals can also be prepared by vibration, sonication or spin coating, where shearing force and surface tension are responsible for the arrangement of particles.[4] In some cases, the highly charged or magnetic particles can be assembled by electric field or magnetic field, and the Coulumbic interaction[5] or magnetic interaction[6] is believed to be the driving force. When the colloidal solution is encapsulated in a small space such as the vesicle in emulsion, its confinement effect may favour the assembly either.[7] Since all these methods have both advantages and disadvantages, the investigation of new method to produce photonic crystals with large size, flexible shapes and high order degree is always desired.

In this work, photonic crystal films are prepared by precipitation of colloidal crystal seeds in particles' supersaturated solution, followed by crystal growth and structure fixing with photo-polymerization. Although there are some research works about the polymeric photonic crystals,[8] little attention was paid to the polymerization itself as a driving force to assemble the particles into colloidal crystals, because most people believe it's just a means to fix the preformed ordered structures. Here, we proposed the 'polymerization-induced colloidal assembly' (PICA) and proved it to be a major driving force to form colloidal crystals. During the transformation from liquid monomer to solid matrix, the highly concentrated SiO_2 particles are forced to precipitate out of the monomer and agglomerate into colloidal microcrystals in several seconds. The PICA method is capable of producing high quality PC films with ultra-narrow bandgap (10–20 nm full width at half maximum (FWHM)), flexible shapes and curvatures, tunable thickness, and large size (half A4) in very short time. Based on these superior characteristics

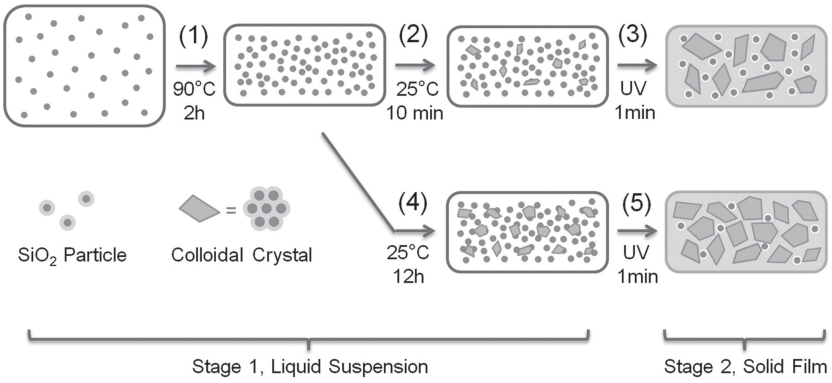

Figure 1. Scheme for the precipitation of colloidal crystals seeds in supersaturated solution of SiO_2 particles (Stage 1) and crystal growth and structure fixing with photo-polymerization (Stage 2).

and the blocking effect of outer PC layer to the reflection of inner layer, we develop a coding-decoding system which translates the reflection spectra of a specific multilayer PC film into an exclusive 'code string' for the identification of the film's composition and stacking sequence. It is believed that the PICA not only reveals a new strategy for colloidal assembly, but also has its value in applications like photonic printing, antifraud and security identification or optical devices.

2. Results and Discussion

The synthesis of colloidal crystal film was accomplished through a preparation of crystal seeds in particle's supersaturated solution, followed by a crystal growth and structure fixing with photo-polymerization. As shown in **Figure 1**, the 1st step is concentration of SiO_2 particles by thermal evaporation and precipitation of particles in their supersaturated solution to form colloidal crystal seeds. Typically, diluted particles (volume fraction, Φ = 0.05) are originally well dispersed in the mixture of ethanol, photo-initiator and acrylate monomer, which could be trimethylolpropane ethoxylate triacrylate (EPTPA), poly(ethylene glycol) diacrylate (PEGDA), poly(ethylene glycol) methacrylate (PEGMA), 2-hydroxyethyl methacrylate (HEMA), methyl methacrylate (MMA) or their mixtures. Ethanol will evaporate after heating the mixture at 90 °C for 2 h, leaving behind a supersaturated acrylate solution of particles, where Φ will increase to about 0.3. As the liquid suspension is cooled down to 25 °C and kept steady for 10 min, a small fraction of particles will precipitate out of the monomer due to supersaturation, forming a mixture of tiny colloidal crystals seeds and highly concentrated particles. If the liquid suspension was placed at 25 °C without disturbance for 12 h, more crystal seeds formed. But longtime placement was still unable to precipitate all the particles, and the suspension was still in liquid form. The 2nd step is colloidal assembly and solidification induced by photo-polymerization. The precursor was sandwiched between two glass slides and converted to a polymeric PC film under UV irradiation immediately. At this moment, the volume of liquid phase gradually decreased to zero and all the particles were forced to precipitate out and assemble into colloidal crystals, which were also fixed in polymer in very short time. It's worth mentioning that both the ethanol evaporation and the storage of precursor should be strictly operated in the dark, as the photo polymerization could be triggered by sunlight or even bulb light, which seriously decrease the fluidity of the precursor and affect the assembly process.

Through a set of verifications, we find that the formation of ordered structure was majorly achieved by PICA in Stage 2, which reveals a new strategy for colloid assembly. In the past few years, similar process has been reported to produce photonic balls or films,[7b] and people tend to believe that SiO_2 particles first form FCC structures during the concentration process in polar acrylate, and the following photo polymerization merely fix the ordered structures. In fact, only a small proportion of SiO_2 particles form colloidal microcrystals after ethanol evaporation, while most of them still have Brownian motion even they are highly concentrated (Φ ~ 0.3) in solution. That explains why the mixing of two independent SiO_2 particle/acrylate precursors with different SiO_2 particles size didn't lead to two strong reflections but one broad and weak reflection after curing (Supporting Information, Figure S1) Once the polymerization begins, liquid monomer quickly solidifies and particles homogeneously precipitate into colloidal microcrystals or deposit onto preformed crystal seeds. The crystal growth was stopped as soon as the critical viscosity for particle moving was reached, and a solid film embedded with numerous colloidal microcrystals forms. **Figure 2** showed the whole process of colloidal assembly and fixing in Stage 2. The liquid precursor sandwiched by cover glasses was placed under microscope and an optical fiber was used to cast UV light on it. The almost colorless precursor gradually turned green after the sample was illuminated for 50 s, which directly proved the colloidal assembly is majorly driven by polymerization.

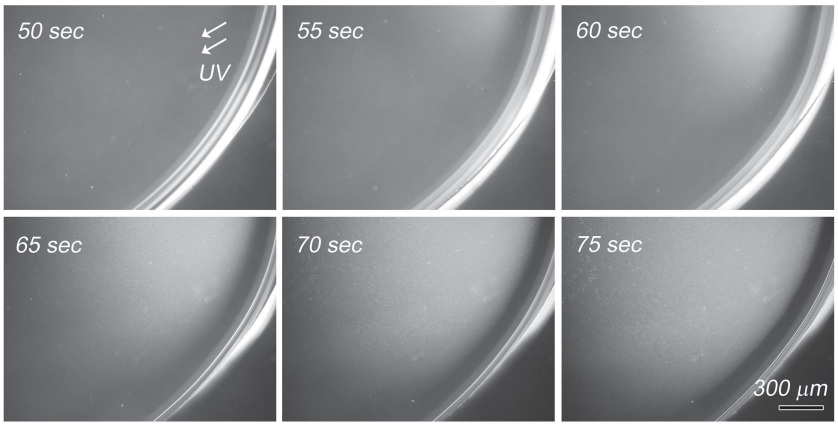

Figure 2. In-situ recording colloidal assembly and fixing using CCD camera on microscope.

In order to further prove PICA is the major reason for colloidal assembly, we compare the color and reflection of seed solution before UV irradiation and PC film after UV curing (SI, Figure S2). As the colloidal crystals effectively reflect visible light, the appearance of brilliant structural color or strong reflection peak could be reliable criteria to confirm the colloidal assembly. When the concentrated solution of particles was placed for 5 min, very pale green color and a weak reflection can be observed, suggesting a small fraction of particles form tiny colloidal crystals seeds. After UV curing, much dense green color and strong reflection with enhancement of 13.2 times can be observed, which indicate most of the particles assemble into colloidal crystals in this step. In a parallel experiment, when the same concentrated solution of particles was placed for 12 h, a noticeable green color and a sharp reflection were obtained, which shows more particles indeed gradually precipitate out of the solution to form more and larger crystals seeds after longtime placement. However, still not all of them were assembled because UV curing leads to an even brighter green color and stronger reflection with enhancement of 6.2 times, which proves PICA again. Generally, the major driving force for colloidal assembly should be the one which assemble most of the particles into colloidal crystals. The appearance of structural color and reflection peaks proves that both precipitation due to supersaturation in Stage 1 and photopolymerization in Stage 2 will induce colloidal assembly, but PICA is always the major driving force.

Polymerization induced colloidal assembly (PICA) is intrinsically different from traditional evaporation induced colloidal assembly (EICA). In EICA, particles are generally dispersed in one or several volatile solvents with low viscosity, and particle precipitation to form crystal seeds and colloidal crystal growth are achieved almost synchronously, because both of them are induced by solvent evaporation. However, in PICA, the seed formation and crystal growth are separated into two independent steps, that is using evaporation of partial solvent to form particles' supersaturated solution and colloidal crystals seeds (Stage 1), and using polymerization to realize the crystal growth (Stage 2). Once partial solvent was evaporated at the beginning of the synthesis, the particles are dispersed in a nonvolatile and viscous liquid monomer, so that evaporation will barely has any influence upon colloidal assembly in latter procedures. Apparently, compared to traditional EICA, the independent control of colloidal crystal seeds and crystal growth will make the PICA process more flexible, controllable and efficient.

In the following discussions, we would explore various parameters in colloidal crystal seed formation and crystal growth, such as ethanol evaporation speed, particle volume fraction and polymerization conditions, which indirectly or directly affect the PICA process. First of all, the ethanol residual in SiO_2 particle/acrylate precursors is an essential condition for producing colloidal crystal seeds. We prepared a mixture of SiO_2 particles (60 μL), PEGDA (140 μL) and ethanol (1000 μL), and carefully calculated the volume of ethanol residuals during the evaporation according to the weight loss of the mixture (**Figure 3**). The same mixture was evaporated at 60 °C and 90 °C for 12 and 2 h, both of which proved there is about 14 μL of ethanol left in the final precursor solution. These ethanol molecules are important for the stabilization of SiO_2 particles, because we have tried to disperse vacuum-dried SiO_2 particles in acrylate monomer, and they didn't dissolve at all. Due to the strong affinity between ethanol and surface Si-OH of silica, the ethanol residuals maybe enriched around the colloids to form a thin solvation layer. Then, the ionization of Si–OH in ethanol causes the particles negative charge on the surface, ensuring the successful colloidal assembly later. In experiments, we did observe a decrease of order degree after

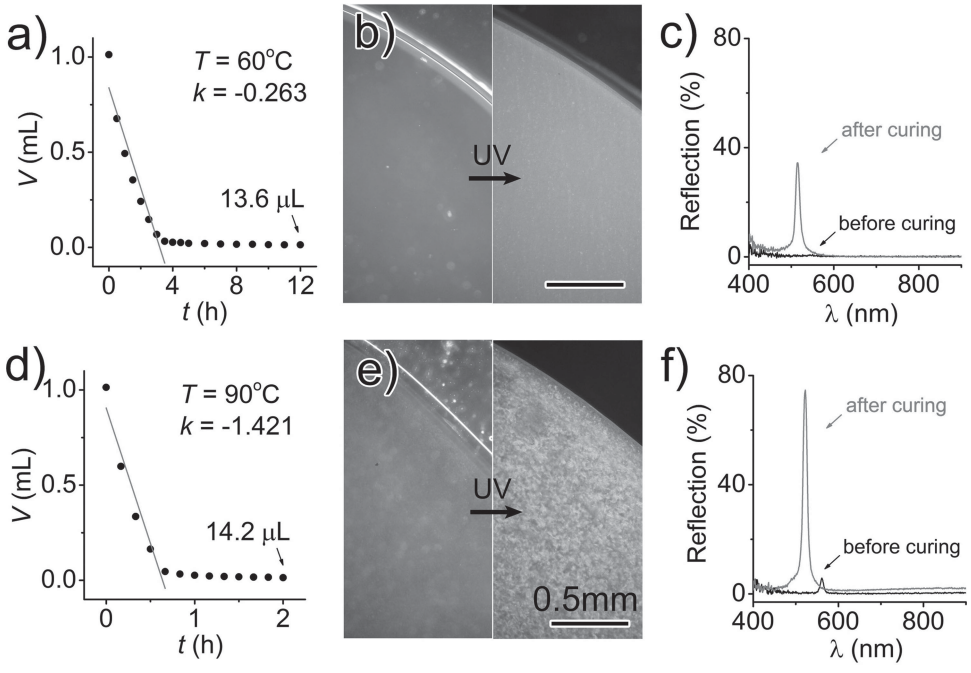

Figure 3. Time evolution of ethanol residuals for evaporation at a) 60 °C and d) 90 °C. Microscopic images and reflection spectra of liquid precursor prepared at b,c) 60 °C and e,f) 90 °C and those of the corresponding cured PC films.

assembly when ethanol was overly evaporated (SI Figure S3) or a few acrylate with ionic groups was introduced (SI Figure S4), which suggested repulsion played an important role in PICA just as it did in other reported assembly process.

The ethanol evaporation speed controls the formation of colloidal crystal seeds, which indirectly determine the colloidal assembly in PICA. For SiO_2 particle/PEGDA precursor evaporated at 60 °C, there are no visible microcrystal seeds and no reflection peak either before polymerization. However, for the same precursor concentrated at 90 °C, many microcrystals appear as green dots (approximately several μm) after 10 min placement and a reflection with intensity of 5.9 was observed, which shows a small proportion of SiO_2 particles does precipitate into colloidal microcrystals at high temperature. Apparently, faster ethanol evaporation rate (0.263 mL/h at 60 °C, 1.421 mL/h at 90 °C) lead to more and larger colloidal crystal seeds. After UV curing, the PC film made from 60 °C precursor is homogeneous green film, and that from 90 °C precursor is composed of bright and larger green zone, which are colloidal microcrystals with very few defects inside (SI, Figure S5). Two groups of microscope images before and after polymerization probably show a homogeneous nucleation and a seeding growth in PICA respectively. For precursor prepared at low temperature, the colloids homogeneously agglomerate into colloidal microcrystals and further grow to small microcrystals in UV curing because there is no seed in monomer. For precursor treated at high temperature, most particles deposited onto the pre-formed seeds and grow into large microcrystals in UV curing, so that the PC film has more intense reflection than the former.

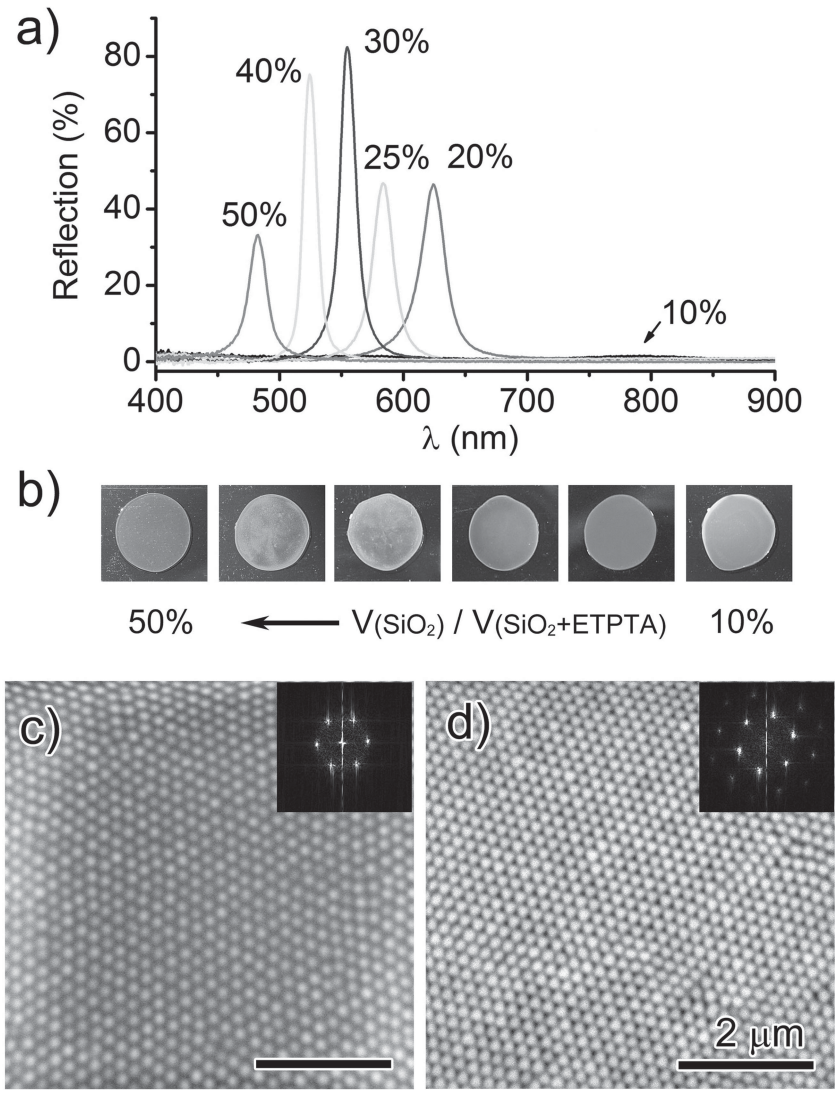

Figure 4. a) The reflection peak of PC film blue-shifts as the volume fraction of SiO_2 particles increases, and b) its color changes from red to blue accordingly. SEM images and FFT patterns of PC films consisted of c) 20% and d) 50% of SiO_2 particles.

Since PICA require the building blocks stay in a short distance, a high particle volume fraction (Φ) is necessary for fast assembly. For the convenience of discussion, the designed particle volume fractions (Φ = 10 ~ 50%) are discussed below. If the volume of ethanol residual is counted in, the practical Φ will be less. PICA can't happen when the volume fraction of SiO_2 particles is below 10%. It's not surprising to see the color changing from red to blue due to the approaching of neighboring particles and thereby the decreasing of lattice constant, when the volume fraction gradually increases from 20% to 50% (**Figure 4**a,b). However, it is interesting to find the as-prepared PC film have very narrow reflection peak. The FWHM are measured to be 10–20 nm in average, which is comparable to that of PC with ultra-narrow reflection in recent reports.[9] The narrow and intense reflection peak proves that the order degree of colloid crystals is very high, even the assembly is accomplished in several seconds.

Except for the wavelength shift tuned by volume fraction, the reflection intensity also present an optimal value around 30%, which suggested that PICA has a best efficiency with such precursors. When the volume fraction is less than 10%, the interspacing of particles is too large to give adequate strong repulsion between them and the particles are free to move during the polymerization, both of which cause the disorder arrangement of particles inside cured acrylate. When the volume fraction gets higher, it becomes "crowded" for the particles inside precursor solution, so that the repulsion increases and most particles are only movable in a small range around the final equilibrium point, which makes it possible for the polymerization to assemble and fix the colloids in a short time. An extremely high volume fraction will be disadvantageous to the assembly either, because there will be no room for the particles to adjust their positions to form the best stacking structures. Therefore, the reflection of PC film made by 50% SiO_2 particle/

acrylate precursor turns slightly weaker and broader. The scanning electron microscope (SEM) images of two typical samples with volume fraction of 20% and 50% are shown in Figure 4c and 4d respectively. The inset Fast Fourier Transformation (FFT) pattern (amplified by 4 times) proves the stacking is ordered. A particle interspacing of 51 and 29 nm can be obtained by subtracting the average SiO_2 particle size (173 nm) from the neighboring core–core distance. Even using the precursor with extreme high particle content (50%), there still exist 29 nm interspacing, which demonstrate the strong repulsion between colloids and presence of solvation layer composed of ethanol and acrylate around the particles.

Polymerization conditions tuning the solidification and particle precipitation rate have direct influence upon the colloidal assembly, as the colloidal crystals form exactly due to the precipitation of particles in liquid-to-solid transition of monomers. Here, four parallel experiments were designed to verify it in the aspects of irradiation strength, photo-initiator, monomer and crosslinking, in which the reflection intensity was utilized to evaluate the order degree of colloidal crystals. (**Figure 5**, SI Figure S6) First, the same precursor was treated with sunlight, weak (4.8 mW/cm^2) and strong (20 mW/cm^2) UV irradiation, respectively. The precursor cured by sunlight in several minutes has the best intensity, while that instantly cured by strong UV has the lowest intensity; because a powerful UV source induce faster solidification and particle precipitation, so that the particles don't have adequate time to form ordered structures before they were fixed. Similarly, excessive photo-initiator in precursor is also disadvantageous to the colloid assembly due to unmatched fast solidification compared to the self-assembly. Furthermore, it was found that SiO_2 particles assembled amazingly well in PEGDA-258, and its reflection intensity has a 7.6 time enhancement compared to that of PEGDA-700. Here, long-chain PEGDA-700 solidified much faster than short-chain PEGDA-258, so that particle precipitate faster and colloidal assembly is worse in former case. For the same reason, Pure ETPTA (100% crosslinker) solidified faster than the mixture of ETPTA and MMA (1:1), so the one with less crosslinking lead to better assembly. These four experiments prove again that the colloid assembly is caused and affected by polymerization, and slow solidification and slow particle precipitation will lead to better colloid assembly and higher reflection intensity.

The good fluidity of SiO_2 particle/acrylate precursor, the fast curing characteristics as well as the in-situ polymerization induced colloidal assembly makes the above process a convenient and efficient method to fabricate photonic crystal films with expected sizes, shapes, or thicknesses. There have been some nice works utilizing this material to prepare photonic balls by microfluidic apparatus. But in this work, we extended the material to the fabrication of photonic crystal multilayer films. If a single layer PC film with a characteristic photonic bandgap can be represented by an independent code, a multilayer PC film can be identified by a code string, which actually reveals the film's composition and stacking sequence. Follow the code string one can prepare the specific multilayer PC, while its reflection spectra can be decoded to give the code string, which establish a new coding-decoding system based on photonic crystals.

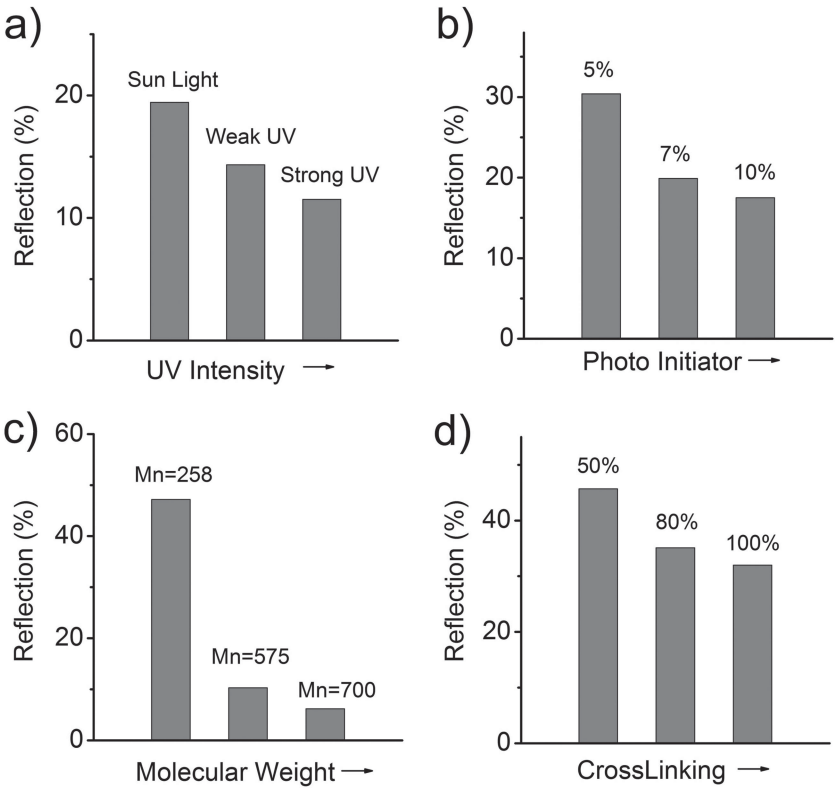

Figure 5. The order degree of photonic structures, represented by the reflection intensity, is affected by a) the strength of UV irradiation, b) the amount of photo initiator, c) the molecular weight of monomer and d) the crosslink level of polymer matrix.

For a single layer PC film with only one bandgap, its reflection intensity and transparency were tightly related to the film thickness. There is a remarkable phenomenon that the thin PC films usually have brilliant colors but the PC blocks with three dimensions in the scale of millimeter seems like an opaque silicone rubber with pale colors. As the thickness increases to millimeter scale, the film is opaque and many defects appear in the path of transmitted light, so that the back scattering light enhances in all wavelengths, the structure color turns weak and the intrinsic white color of polymer appears. On the other hand, with the thickness decreased, the film becomes more transparent but less colourful either, because the number of periodic structures decreases. Through the control of intervals in synthesis, PC films with different thickness (SI, Figure S7) can be prepared, and their reflections first enhance then drop as the film turns thicker. (**Figure 6**a,b) An optimal thickness around 60 μm can be achieved, which reveals a suitable thickness

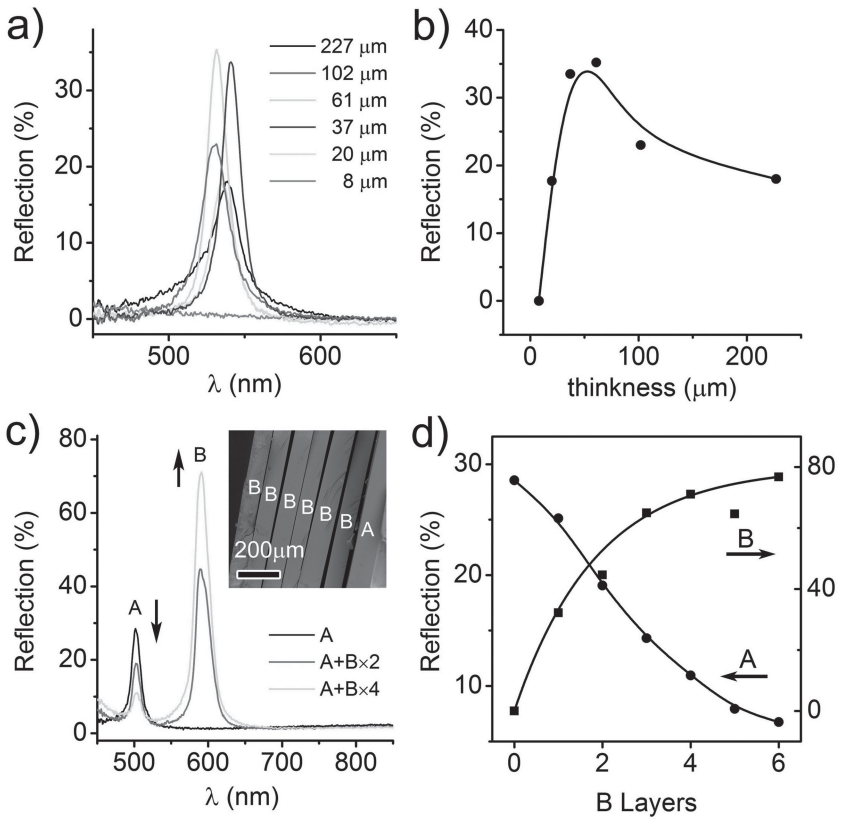

Figure 6. a,b) Independence of reflection intensity upon the thickness of single component layer and c,d) evolution of reflection *A* and *B* as layer *B* was stacked upon *A* one by one.

for PC film possessing both intense reflection and good transparency.

For a multilayer PC film with several distinguishable bandgaps, the overall reflection spectra was determined by not only the thickness but also the stacking sequence of each layer. First, we prepared a multilayer PC film with only two components, layer *A* and *B*, which reflects visible light at 500 and 587 nm respectively. Layer *A* was first fixed on a glass slide while layer *B* was stacked upon *A* one by one, and each layer was controlled to have an average thickness of 84 μm. Reflection spectra were then recorded every time a new layer was fixed on the previous sample. (The gaps between each layer are caused by the breaking of film in order to observe its cross-section in SEM). In the beginning when no *B* layer was covering outside, the film only has reflection *A* with intensity around 30. As 6 layers of films *B* stacked upon film *A* in sequence, the intensity *A* decrease to 7 and intensity *B* increase to 80 instead. (Figure 6c,d) The falling of reflection *A* suggested the outer PC films have blocking effect to the reflection signal from inner layers, because both the incident light illuminating the inner layer and the reflected light emitting from the inner layer were weakened due to the scattering of outer layers. For the same reason, the intensity *B* will not increase linearly as the layer increase but gradually reaches a saturated value. This experiment demonstrated the essentialness of high transparency and intense reflection for a single PC film component. Otherwise, the reflection from inner layer will be too weak to be observed and quantified. It also indicated the importance of narrow bandgap for multilayers so that the reflection peaks of every layer won't interfere with each other and the change of intensities are easy to be understood and predicted.

Based on the blocking effect of outer layer, we developed a coding and decoding system which utilize the reflection wavelength and peak area to identify the composition and stacking sequence of multilayer PC film, thus translating the reflection spectra into distinctive code strings. As shown in **Figure 7**, three SiO_2 particle/acrylate precursors and triple layer structures are chosen for the demonstration. Because each layer can be prepared by any of the 3 precursor, there will be 27 combinations or code strings in total. Here, the code string is defined by three alphabets, such as ABC, which means in the corresponding film, *A* is the inner layer, *B* is in the middle and *C* is the outer layer. When the triple layer is composed of same precursor (*A* or *B* or *C*), the reflection spectra shows a single peak equalling to that of single layer with triple thickness. When it is prepared by two components (*A* and *B*), the ratio of peak area (*A*:*B*) increases as the layer *A* moving outside. For multilayer consisted of three components (*A*, *B* and *C*), a qualitatively conclusion can be drawn that the outer layer has largest peak area, and the middle and inner layer has middle and smallest peak area respectively. These results suggested that the layer sequence expressed by code strings can be carried by the reflection spectra.

In order to realize the decoding functions, a quantitative data processing method must be developed to precisely convert each reflection spectra into layer sequence (or code strings). Since the light intensity is in proportion to the reflection peak area (S_A, S_B and S_C), one can estimate the contribution in reflection at each wavelength by calculating its percentage among the total area (S_A/S_T, S_B/S_T and S_C/S_T, $S_T = S_A + S_B + S_C$). **Figure 8** showed the statistical treatment of reflection spectra of 3 triple layer PC film, and the data from all the combinations can be summarized into a decoding table (**Table 1**). The percentages around 20%, 30%, and 40% indicate that this film is located in the bottom, middle and upper layer, respectively. Higher percentages may appear when some layers are using the same material. Taking the 1st sample in Figure 8 as an example, its S_A/S_T, S_B/S_T and S_C/S_T are calculated to be 24.68, 30.33, and 44.98% according to the original reflection spectra, so that the layer sequence and the code string can be determined as "ABC" from the decoding table. These films are hard to distinguish by naked eye, but with the help of decoding table, one can easily determine their layer sequence by measuring their reflections. In theory, additional codes can be added to the system only if their reflection peak shift 50 nm from the current one considering an average FWHM of 25 nm for such PC film, which means 6 codes can be used in the visible range from 450 to 700 nm. A coding system composed of 6^6 (46656) codes is

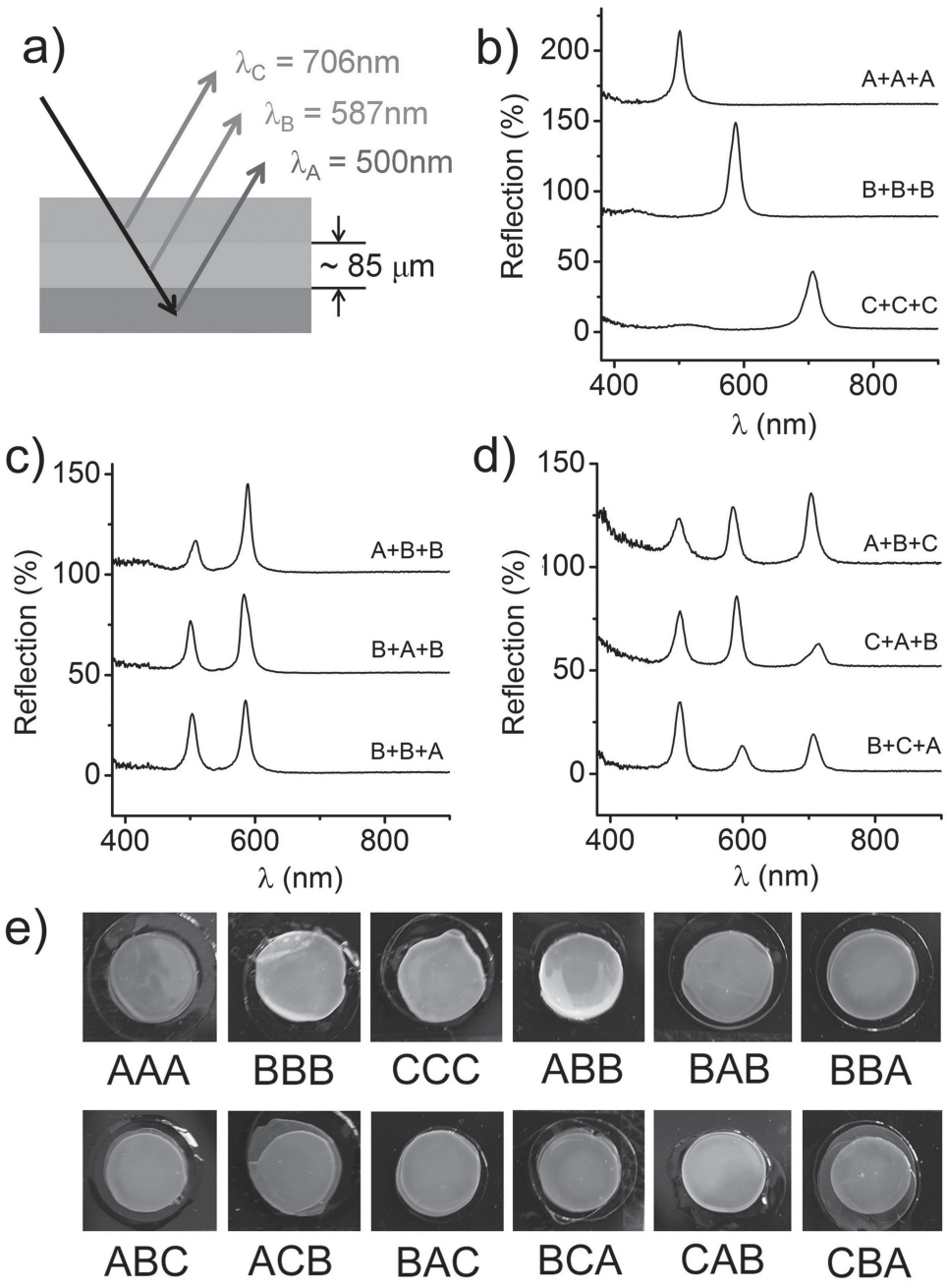

Figure 7. a) Scheme, b–d) reflection spectra and e) photos of triple layer PC films stacked with different sequences. A+B+C or ABC means *A* is the inner layer, *B* is in the middle and *C* is the outer layer.

fascinating, but the difficulty in determination of the sequence of most inner layers also increases due to their relative lower reflection intensities, so that a more accurate control must be taken in the synthesis.

3. Conclusions

Photonic crystal films are prepared by precipitation of colloidal crystal seeds in particles' supersaturated solution, followed by a crystal growth and structure fixing with photo-polymerization. PICA was proved to be the major driving force to form colloidal crystals. As the liquid monomer turns to solid matrix, the highly concentrated particles are forced to precipitate into colloidal microcrystals in short time. PICA is intrinsically difference from evaporation induced colloidal assembly, since the seed formation and crystal growth are separated into two independent steps, which makes the synthesis more flexible, controllable and efficient. The ethanol evaporation speed, the particle volume fraction in precursor and polymerization

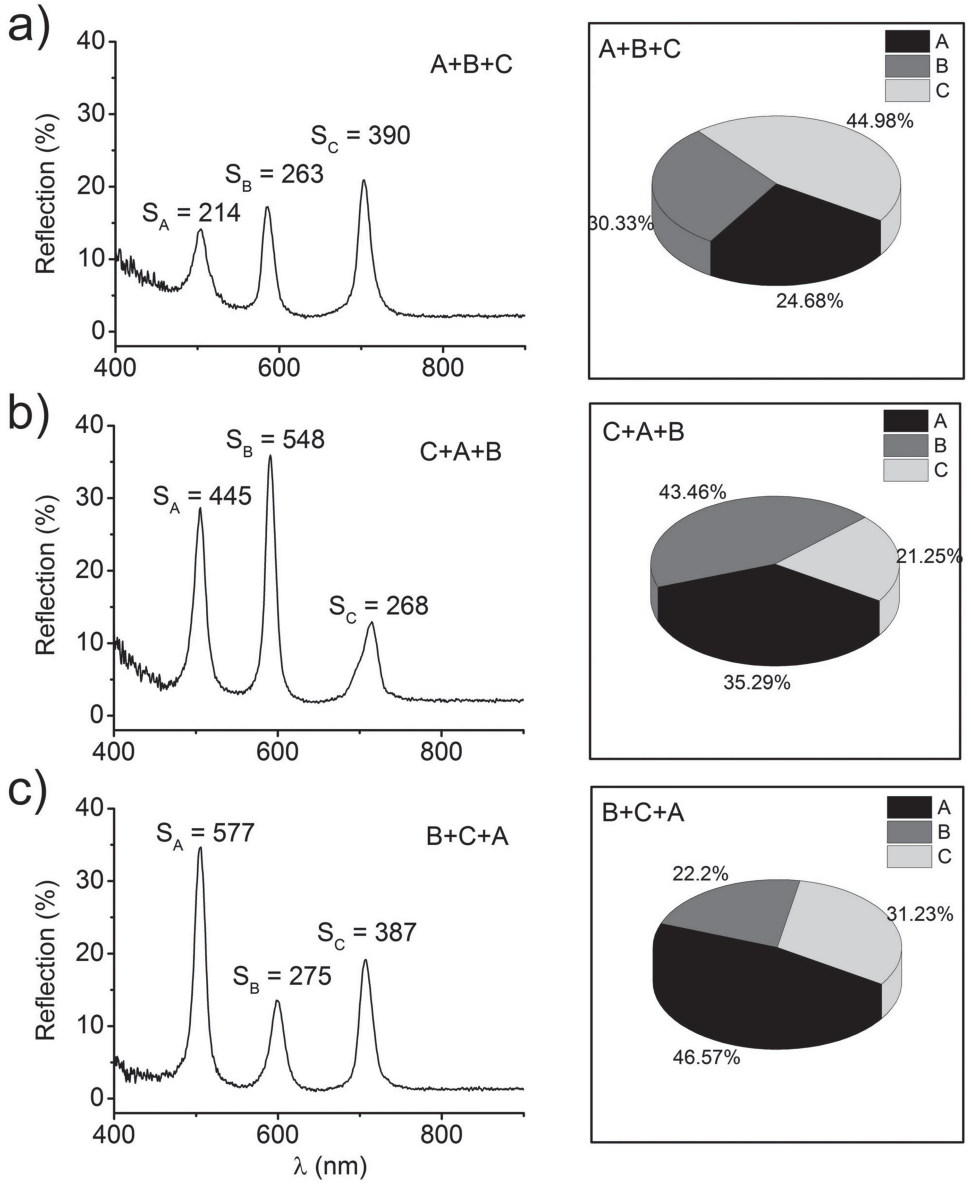

Figure 8. Original reflection spectra and statistics of reflection contributions of triple-layer PC films stacked in the sequence of a) ABC, b) CAB, and c) BCA.

conditions affecting the particle precipitation rate all control the order degree of colloidal crystals. The PICA process is capable of fast producing PC films with ultra-narrow bandgap, tunable thickness and large size. Based on these superior characteristics and the blocking effect of outer PC layer to the reflection of inner layer, we develop a coding-decoding system so that the film's composition and stacking sequence, represented by a code string, can be identified or decoded by its reflection spectra. PICA reveals a new strategy to prepare composite photonic structures, and maybe further used in photonic printing, security identification and optical devices.

Table 1. Decoding table of triple layer photonic crystal films, whose stack sequence can be deduced from the percentage of peak area (S_A, S_B, and S_C) at each wavelength.

	S_A/S_T [%]	S_B/S_T [%]	S_C/S_T [%]		S_A/S_T [%]	S_B/S_T [%]	S_C/S_T [%]
AAA	100	-	-	ABC	24.68	30.33	44.98
BBB	-	100	-	ACB	21.48	46.97	31.54
CCC	-	-	100	BAC	36.37	21.8	41.82
ABB	26	74	-	BCA	46.57	22.2	31.23
BAB	35	65	-	CAB	35.29	43.46	21.25
BBA	46	54	-	CBA	44.85	36.58	18.57

4. Experimental Section

Materials: 2-Carboxyethyl acrylate, poly(ethylene glycol) methacrylate (PEGMA, Mn = 360), poly(ethylene glycol) diacrylate (PEGDA, with different molecular weight Mn = 250, 575, 700) and trimethylolpropane ethoxylate triacrylate (ETPTA, Mn = 428) were purchased from

Sigma-Aldrich. Methyl methacrylate (MMA, 99.8%) and 2-hydroxy-2-methylpropiophenone (96%) were purchased from TCI Co. Ltd. tetraethylorthosilicate (TEOS, 98%), and ammonium hydroxide solution (28%) were purchased from Sinopharm Chemical Reagent Co. 2-Hydroxyethyl methacrylate (HEMA, 99%) and ethanol (99.9%) were purchased from J&K. All chemicals were used directly as received without further treatment.

Preparation of SiO_2 Particle/Acrylate Precursors: Monodisperse SiO_2 particles with diameters ranged from 130 to 200 nm were synthesized by Stöber method. The SiO_2 particles were dispersed in ethanol by sonication and then mixed with acrylate (such as ETPTA, PEGDA, PEGMA) containing photo initiator, 2-hydroxy-2-methylpropiophenone (5%). The total volume of the mixture was fixed at 1.2 mL before ethanol evaporation, which contained 0.2 mL of SiO_2 particles and acrylate in designed proportions. The solution containing the SiO_2 particles was homogenized by vortex mixing and sonication, and transferred to an oven at 60 °C. After 12 h of ethanol evaporation in the oven, a transparent precursor solution was obtained and kept in dark place before usage.

Fabrication of Photonic Crystal Films: Typically, precursor solution (30 µL) was sandwiched between a glass slides and a piece of hydrophobic cover glass. The thickness of the film can be controlled by altering the thickness of interval objects separating the two glass slides. After being exposed to UV light (365 nm, 4.8 mW/cm^2) for 5 s, the liquid precursor was polymerized and the colorful photonic crystal films with approximate thickness of 180 µm were obtained. In the fabrication of multilayer films, precursor solution (10 µL) was dropwise added to a pre-made photonic crystals film for further polymerization. This curing process was repeated until the expected layer number was achieved.

Characterization: The average size of the SiO_2 particles was determined by a JEOL JEM-2100 transmission electron microscope. The assembly of SiO_2 particles within the photonic crystals film was observed by a Phenom G2 Pro scanning electron microscope. The optical microscope images were taken by an Olympus BXFM reflection-type microscope operated in dark-field mode. The reflection spectra were measured by an Ocean Optics Maya 2000 Pro spectrometer coupled to a six-around-one reflection/back scattering probe, where both the incident and reflective angle were fixed at 0°.

Supporting Information

Supporting Information is available from the Wiley Online Library or from the author.

Acknowledgements

J. Ge thanks the support from Major State Basic Research Development Program of China (2011CB932404), National Science Foundation of China (21001083, 21222107), Shanghai Rising-Star Program (13QA1401400).

Received: May 09, 2013
Revised: July 05, 2013
Published online: August 19, 2013

[1] a) Y.-J. Zhao, X.-W. Zhao, J. Hu, J. Li, W.-Y. Xu, Z.-Z. Gu, *Angew. Chem. Int. Ed.* **2009**, *48*, 7350–7352; b) E. Tian, J. Wang, Y. Zheng, Y. Song, L. Jiang, D. Zhu, *J. Mater. Chem.* **2008**, *18*, 1116–1122; c) A. C. Arsenault, T. J. Clark, G. Von Freymann, L. Cademartiri, R. Sapienza, J. Bertolotti, E. Vekris, S. Wong, V. Kitaev, I. Manners, R. Z. Wang, S. John, D. Wiersma, G. A. Ozin, *Nat. Mater.* **2006**, *5*, 179–184; d) A. C. Arsenault, D. P. Puzzo, I. Manners, G. A. Ozin, *Nat. Photonics* **2007**, *1*, 468–472; e) H. Kim, J. Ge, J. Kim, S.-e. Choi, H. Lee, H. Lee, W. Park, Y. Yin, S. Kwon, *Nat. Photonics* **2009**, *3*, 534–540; f) F. Li, D. P. Josephson, A. Stein, *Angew. Chem. Int. Ed.* **2011**, *50*, 360–388.

[2] a) H. Miguez, F. Meseguer, C. Lopez, A. Blanco, J. S. Moya, J. Requena, A. Mifsud, V. Fornes, *Adv. Mater.* **1998**, *10*, 480; b) A. Rogach, A. Susha, F. Caruso, G. Sukhorukov, A. Kornowski, S. Kershaw, H. Mohwald, A. Eychmuller, H. Weller, *Adv. Mater.* **2000**, *12*, 333; c) R. C. Schroden, M. Al-Daous, C. F. Blanford, A. Stein, *Chem. Mater.* **2002**, *14*, 3305–3315.

[3] a) A. S. Dimitrov, K. Nagayama, *Langmuir* **1996**, *12*, 1303–1311; b) P. Jiang, J. F. Bertone, K. S. Hwang, V. L. Colvin, *Chem. Mater.* **1999**, *11*, 2132–2140; c) Z. Z. Gu, A. Fujishima, O. Sato, *Chem. Mater.* **2002**, *14*, 760–765; d) V. Rastogi, S. Melle, O. G. Calderon, A. A. Garcia, M. Marquez, O. D. Velev, *Adv. Mater.* **2008**, *20*, 4263–4268; e) M. H. Kim, S. H. Im, O. O. Park, *Adv. Mater.* **2005**, *17*, 2501.

[4] a) S. H. Park, D. Qin, Y. N. Xia, *Adv. Mater.* **1998**, *10*, 1028; b) O. Vickreva, O. Kalinina, E. Kumacheva, *Adv. Mater.* **2000**, *12*, 110–112; c) P. Jiang, M. J. McFarland, *J. Am. Chem. Soc.* **2004**, *126*, 13778–13786; d) D. Y. Wang, H. Mohwald, *Adv. Mater.* **2004**, *16*, 244; e) S. Reculusa, S. Ravaine, *Chem. Mater.* **2003**, *15*, 598–605.

[5] a) S. O. Lumsdon, E. W. Kaler, J. P. Williams, O. D. Velev, *Appl. Phys. Lett.* **2003**, *82*, 949–951; b) R. Xie, X.-Y. Liu, *J. Am. Chem. Soc.* **2009**, *131*, 4976–4982; c) J. R. Millman, K. H. Bhatt, B. G. Prevo, O. D. Velev, *Nat. Mater.* **2005**, *4*, 98–102.

[6] a) X. L. Xu, G. Friedman, K. D. Humfeld, S. A. Majetich, S. A. Asher, *Adv. Mater.* **2001**, *13*, 1681–1684; b) J. Ge, Y. Hu, Y. Yin, *Angew. Chem. Int. Ed.* **2007**, *46*, 7428–7431; c) T. Ding, K. Song, K. Clays, C.-H. Tung, *Adv. Mater.* **2009**, *21*, 1936–1940.

[7] a) S.-H. Kim, S. Y. Lee, G.-R. Yi, D. J. Pine, S.-M. Yang, *J. Am. Chem. Soc.* **2006**, *128*, 10897–10904; b) S.-H. Kim, S.-J. Jeon, G.-R. Yi, C.-J. Heo, J. H. Choi, S.-M. Yang, *Adv. Mater.* **2008**, *20*, 1649; c) Y. Zhao, Z. Xie, H. Gu, L. Jin, X. Zhao, B. Wang, Z. Gu, *Asia Mater.* **2012**, 4, e25.

[8] a) Y. J. Zhao, X. W. Zhao, J. Hu, M. Xu, W. J. Zhao, L. G. Sun, C. Zhu, H. Xu, Z. Z. Gu, *Adv. Mater.* **2009**, *21*, 569; b) S. A. Asher, J. Holtz, L. Liu, Z. Wu, *J. Am. Chem. Soc.* **1994**, *116*, 4997–4998; c) L. L. Duan, B. You, S. X. Zhou, L. M. Wu, *J. Mater. Chem.* **2011**, *21*, 687–692; d) S. H. Kim, S. Y. Lee, S. M. Yang, G. R. Yi, *Asia Mater.* **2011**, *3*, 25–33; e) R. Goldberg, H. J. Schope, *Chem. Mater.* **2007**, *19*, 6095–6100; f) Y. J. Zhao, X. W. Zhao, B. C. Tang, W. Y. Xu, Z. Z. Gu, *Langmuir* **2010**, *26*, 6111–6114; g) Y. D. Hu, J. Y. Wang, H. Wang, Q. Wang, J. T. Zhu, Y. J. Yang, *Langmuir* **2012**, *28*, 17186–17192; h) Y. Iwayama, J. Yamanaka, Y. Takiguchi, M. Takasaka, K. Ito, T. Shinohara, T. Sawada, M. Yonese, *Langmuir* **2003**, *19*, 977–980.

[9] Y. Huang, J. Zhou, B. Su, L. Shi, J. Wang, S. Chen, L. Wang, J. Zi, Y. Song, L. Jiang, *J. Am. Chem. Soc.* **2012**, *134*, 17053–17058.